ORIGINAL PAPER

A new optimal root-finding iterative algorithm: local and semilocal analysis with polynomiography

Sania Qureshi[1,2,3] (ID) · **Ioannis K. Argyros**[4] (ID) · **Amanullah Soomro**[1] (ID) ·
Krzysztof Gdawiec[5] (ID) · **Asif Ali Shaikh**[1,2] (ID) · **Evren Hincal**[2] (ID)

Abstract

In this work, a new optimal iterative algorithm is presented with fourth-order accuracy for root-finding of real functions. It uses only function as well as derivative evaluation. The algorithm is obtained as a combination of existing third-order methods by specifying a parameter involved. The algorithm is based on local and semilocal analysis and has been specifically designed to improve efficiency and accuracy. The proposed algorithm represents a significant improvement over existing iterative algorithms. In particular, it is tested on a range of polynomial functions and was found to produce accurate and efficient results, with improved performance over existing algorithms in terms of both speed and accuracy. The results demonstrate the effectiveness of the proposed algorithm and suggest that it has great potential for use in a wide range of applications in polynomiography and other areas of mathematical analysis.

Keywords Root finding · Fourth-order method · Local and semilocal analysis · Polynomiography

1 Introduction

Numerical methods play a crucial role in solving non-linear transcendental equations in the field of numerical analysis [13]. These equations, also known as implicit equations, cannot be solved analytically and require the use of iterative techniques to find approximate solutions. One of the most important reasons for using numerical methods to solve non-linear transcendental equations is the ability to handle complex and non-analytic functions. These equations often arise in various fields such as physics, engineering, and economics and cannot be solved using traditional analytical methods. For example, in physics, non-linear equations often describe the behavior of systems

---

✉ Krzysztof Gdawiec
krzysztof.gdawiec@us.edu.pl

Extended author information available on the last page of the article

with multiple interacting components, such as the Navier–Stokes equations in fluid dynamics. In engineering, non-linear equations are used to model the behavior of materials under different loads and conditions. Another important reason for using numerical methods is the ability to handle large systems. Non-linear equations often describe the behavior of systems with many interacting components, and solving them analytically can be extremely difficult, if not impossible. Numerical methods provide a way to break down these large systems into smaller, more manageable parts and find approximate solutions using iterative techniques.

There are several root-finding numerical methods that can be used to solve non-linear transcendental equations, such as fixed-point iteration, the secant method, and the Newton–Raphson method which is one of the most frequently used methods. Each method has its own strengths and weaknesses, and the choice of method will depend on the specific equation being solved and the desired level of accuracy. For example, the bisection method is a simple and robust method for finding roots of a function, but it is relatively slow and may not converge for certain types of functions. The Newton–Raphson method, on the other hand, is faster and more accurate, but it requires the derivative of the function and may not converge for certain types of functions. In addition, the choice of the numerical method also depends on the initial conditions, the interval of the solutions, and the number of solutions.

As a workaround, iterative methods have been developed to locate the initial values of solutions to the non-linear equations in the form as follows:

$$\psi(x) = 0, \tag{1}$$

where ψ is a differentiable operator defined on a non-empty, open convex subset Σ of the real line H with values in itself. Such equations rarely have exact solutions. Slow convergence, non-convergence, divergence, inefficiency, and failure are all issues that researchers using iterative methods must contend with. As a result, scientists all over the world are striving to perfect and create new higher-order multi-point methods that do not rely on the second-order derivative. Theoretically, multi-point methods are better than one-point approaches when it comes to ordering and how well they work with computers.

In this paper, we develop a new fourth-order optimal method for finding simple roots of non-linear equations. It is worth to be noted that an optimal root-finding algorithm, in the sense of the classical Kung–Traub conjecture [15], possesses a convergence order of $2^{\kappa-1}$ where κ stands for the number of function evaluations per iteration. To achieve the optimal order of convergence, the proposed scheme requires only two values of the involved function $\psi(x)$ and one of its first-order derivatives. Our method also has a relatively straightforward structure. When the number of roots is known in advance, we also propose a main theorem that exemplifies convergence to the fourth order. We also show how our method performs numerically on examples drawn from the real world, including the continuous stirred tank reactor (CSTR), Plank's radiation, and the Van der Waals equation of state. To further illustrate the behavior of our methods in comparison to the existing methods, we present numerical and graphical examples.

The rest of the paper is organized as follows. In Section 2, we introduce some well-known root-finding methods that are later used for comparison purposes. Next,

in Section 3, we derive a new root-finding method and prove its convergence. The local analysis of the proposed method is carried out in Sections 4 and 5, whereas in Section 6, we perform the semilocal analysis of the method. Then, in Section 7, we present some examples divided into numerical and graphical examples. Finally, in Section 8, we conclude the paper and give future study directions.

2 Some existing root-finding methods

The importance of root-finding methods can also be seen in the development of new technologies. For example, in the field of control systems, root-finding methods are used to find the solutions of non-linear equations that describe the behavior of the system, enabling the design of control systems that are more efficient and more robust. In numerical optimization, root-finding methods are used to find solutions of equations that describe the behavior of the system, which enables the design of optimization algorithms that are more efficient and robust. In summary, root-finding numerical methods are important because they provide a way to find the solutions of non-linear equations, which often have no closed-form solutions. They are used in a wide range of fields to solve problems that involve non-linear equations and to design new technologies, which makes them essential in many areas of research and development.

There are several classical root-finding methods for solving non-linear transcendental equations in the literature. Some common methods include the following:

1. Bisection method [7]: This is a simple and robust method that involves repeatedly bisecting an interval and determining which subinterval a root lies in.
2. Newton–Raphson method [7]: This method uses an initial guess and an iterative process to converge on a root. It requires the ability to compute the derivative of the function.
3. Secant method [7]: This method is similar to the Newton–Raphson method but uses the slope of the secant line between two points rather than the derivative of the function.
4. Fixed point iteration [7]: This method involves finding the fixed point of a function using an iterative process. It requires the function to be in a specific form.
5. Muller's method [7]: This method is an extension of the secant method, and it is used for complex roots.
6. Aitken's Δ^2 method [7]: This method is used for speeding up the convergence of the fixed-point iteration method.
7. Bairstow's method [16]: This method is used for finding the roots of polynomials with real coefficients, and it is used to find the roots of polynomials of degrees greater than 2.
8. Hybrid method: As the name suggests, this method combines two or more methods to find the root of the non-linear equation. Several hybrid methods exist in the current literature. See, for example, [6, 10, 17, 18] and the references cited therein.
9. Hybrid methods with optimization: Several root-finding algorithms exist that use optimization techniques to reduce computational effort and save machine memory.

A few of such algorithms can be found in [25, 26, 28] and most of the references cited therein.

Given below are some of the root-finding numerical methods that are chosen to be used for the comparative analysis in the present research work. Among all the existing methods, one-step Newton–Raphson comes first with the second-order convergence. Its computational steps are as follows:

$$x_{n+1} = x_n - \frac{\psi(x_n)}{\psi'(x_n)}, \ n = 0, 1, 2, \ldots, \tag{2}$$

where $\psi'(x_n) \neq 0$.

Jisheng et al. in [11] proposed an optimal two-step algorithm (KJNM) with fourth-order convergence as follows:

$$
\begin{aligned}
y_n &= x_n - \frac{\psi(x_n)}{\psi'(x_n)}, \\
x_{n+1} &= x_n - \frac{\psi(x_n)^2 + \psi(y_n)^2}{\psi'(x_n)(\psi(x_n) - \psi(y_n))}.
\end{aligned}
\tag{3}
$$

Ostrowsiki's optimal two-step fourth-order convergent algorithm (OWNM) in [14] is given by the following:

$$
\begin{aligned}
y_n &= x_n - \frac{\psi(x_n)}{\psi'(x_n)}, \\
x_{n+1} &= y_n - \frac{\psi(x_n)\psi(y_n)}{\psi'(x_n)(\psi(x_n) - 2\psi(y_n))}.
\end{aligned}
\tag{4}
$$

Özban in [19] proposed an optimal two-step fourth-order convergent algorithm (OZNM) which is given by the following steps:

$$
\begin{aligned}
y_n &= x_n - \frac{\psi(x_n)}{\psi'(x_n)}, \\
x_{n+1} &= x_n - \frac{\psi(x_n)(\psi'(x_n) + \psi'(y_n))}{2\psi'(y_n)\psi'(x_n)}.
\end{aligned}
\tag{5}
$$

Kung and Traub in [15] proposed an optimal two-step fourth-order convergent algorithm (KTNM) which is given by the following steps:

$$
\begin{aligned}
y_n &= x_n - \frac{\psi(x_n)}{\psi'(x_n)}, \\
x_{n+1} &= y_n - \frac{\psi(x_n)^2\psi(y_n)}{\psi'(x_n)(\psi(x_n) - \psi(y_n))^2}.
\end{aligned}
\tag{6}
$$

3 Construction of the method

In this section, we use the idea of an affine combination of two well-established iterative methods for proposing a new optimal iterative method to deal with non-linear equations of the type (1).

One of the methods proposed by Zhou in [29] is as follows:

$$x_{n+1} = x_n - \frac{\psi(x_n)^2 - 2\psi(x_n)\psi\left(x_n - \frac{\psi(x_n)}{\psi'(x_n)}\right)}{\psi(x_n)\psi'(x_n) - 3\psi'(x_n)\psi\left(x_n - \frac{\psi(x_n)}{\psi'(x_n)}\right)}, \ n = 0, 1, 2, \dots . \quad (7)$$

It is known as a modified version of the Chebychev–Halley method and offers a third-order convergence, while Potra–Pták in [21] proposed a third-order convergent method as follows:

$$x_{n+1} = x_n - \frac{\psi(x_n) + \psi\left(x_n - \frac{\psi(x_n)}{\psi'(x_n)}\right)}{\psi'(x_n)}, \ n = 0, 1, 2, \dots . \quad (8)$$

Our aim is to construct a new optimal fourth-order convergent method by using an affine combination of algorithms given in (7) and (8). The new method takes the following form:

$$x_{n+1} = x_n - \eta \frac{\psi(x_n) + \psi(y_n)}{\psi'(x_n)} - (1 - \eta)\frac{\psi(x_n)^2 - 2\psi(x_n)\psi(y_n)}{\psi(x_n)\psi(x_n)' - 3\psi'(x_n)\psi(y_n)}, \quad (9)$$

where $y_n = x_n - \frac{\psi(x_n)}{\psi'(x_n)}$ and $\eta \in \mathbb{R}$ is the adjusting parameter. When $\eta = 0$, the method reduces to the method (7), and when $\eta = 1$, it gives the method (8). It is noticeable that the methods which are given in (7) and (8) are not optimal while the one in (9) is an optimal fourth-order convergent method, and its performance depends on the parameter η which is obtained from Taylor expansion as given in Theorem 1.

Theorem 1 *Assume that the function $\psi : D \subset \mathbb{R} \to \mathbb{R}$ has a simple root $\gamma \in D$, where D is an open interval. If ψ is sufficiently smooth in the neighborhood of the root γ, then the order of convergence of the iterative method defined by (9) is at least three as shown in the following equation:*

$$(3\eta - 1)c_2^2 e_n^3 + \mathcal{O}(e_n^4), \quad (10)$$

where $e_n = x_n - \gamma$, and $c_r = \frac{\psi^{(r)}(\gamma)}{r!\psi'(\gamma)}$, $r = 2, 3, 4, \dots$. Furthermore, if $\eta = \frac{1}{3}$, then the order of convergence is four.

Proof Let $e_n = x_n - \gamma$ and $d_n = y_n - \gamma$. Expanding $\psi(x_n)$ via Taylor expansion about γ, we obtain

$$\psi(x_n) = \psi'(\gamma)\left[e_n + c_2 e_n^2 + c_3 e_n^3 + c_4 e_n^4 + \mathcal{O}(e_n^5)\right]. \tag{11}$$

Expanding $\psi'(x_n)$ via Taylor expansion about γ, we obtain

$$\psi'(x_n) = \psi'(\gamma)\left[1 + 2c_2 e_n + 3c_3 e_n^2 + 4c_4 e_n^3 + \mathcal{O}(e_n^4)\right]. \tag{12}$$

Dividing (11) by (12), we get

$$\frac{\psi(x_n)}{\psi'(x_n)} = e_n - c_2 e_n^2 + 2(c_3 - c_2^2)e_n^3 + (7c_2 c_3 - 4c_2^3 - 3c_4)e_n^4 + \mathcal{O}(e_n^5). \tag{13}$$

From the above equations, we have

$$d_n = e_n - \frac{\psi(x_n)}{\psi'(x_n)} = c_2 e_n^2 + 2(c_3 - c_2^2)e_n^3 + (4c_2^3 + 3c_4 - 7c_2 c_3)e_n^4 + \mathcal{O}(e_n^5). \tag{14}$$

Now expanding $\psi(y_n)$ about γ, we get

$$\psi(y_n) = \psi'(\gamma)\left(d_n + c_2 d_n^2 + c_3 d_n^3 + c_4 d_n^4 + \mathcal{O}(d_n^5)\right). \tag{15}$$

By using (14), we get the following Taylor expansion of $\psi(y_n)$:

$$\psi(y_n) = \psi'(\gamma)\left(c_2 e_n^2 + 2(c_3 - c_2^2)e_n^3 + (5c_2^3 + 3c_4 - 7c_2 c_3)e_n^4 + \mathcal{O}(e_n^5)\right). \tag{16}$$

Finally, substituting the obtained series for (11)–(13) and (16) into the structure (9), the error equation is obtained as follows:

$$e_{n+1} = (3\eta - 1)c_2^2 e_n^3 + \mathcal{O}(e_n^4). \tag{17}$$

This means that for any $\eta \in \mathbb{R}$, the method defined by (9) is at least cubically convergent. To increase the order of convergence for the method (9), the error equation (17) suggests that the parameter η must be $\frac{1}{3}$. Using this value of η in (9), the optimal proposed method (PONM) takes the following form:

$$y_n = x_n - \frac{\psi(x_n)}{\psi'(x_n)},$$

$$x_{n+1} = x_n - \frac{\psi(x_n)\left(\psi(x_n) - 2\psi(y_n)\right) - \psi(y_n)^2}{\psi'(x_n)\left(\psi(x_n) - 3\psi(y_n)\right)}, \tag{18}$$

while its fourth-order convergence is discussed in the following section.   □

The flowchart of the optimal fourth-order two-step iterative method (18) is shown in Fig. 1.

4 Local convergence analysis: first approach

Local convergence analysis for root-finding methods is a method used to determine the conditions under which a given iterative method can converge to a root of a non-linear equation of the type (1). Specifically, it determines the region of the complex plane around a root where the iterative method will converge. The analysis begins by assuming that the iterative method has converged to a root, and then analyzing the behavior of the method in the vicinity of the root. The analysis typically involves examining the behavior of the method's iteration function, which maps the current estimate of the root to the next estimate. An important tool used in local convergence analysis is Taylor series expansion, which can be used to approximate the iteration function around the root. This approximation can then be used to determine the rate at which the method converges to the root, as well as any conditions that must be satisfied for convergence. The analysis typically involves determining the radius of convergence, which is the distance from the root at which the iteration function can be approximated
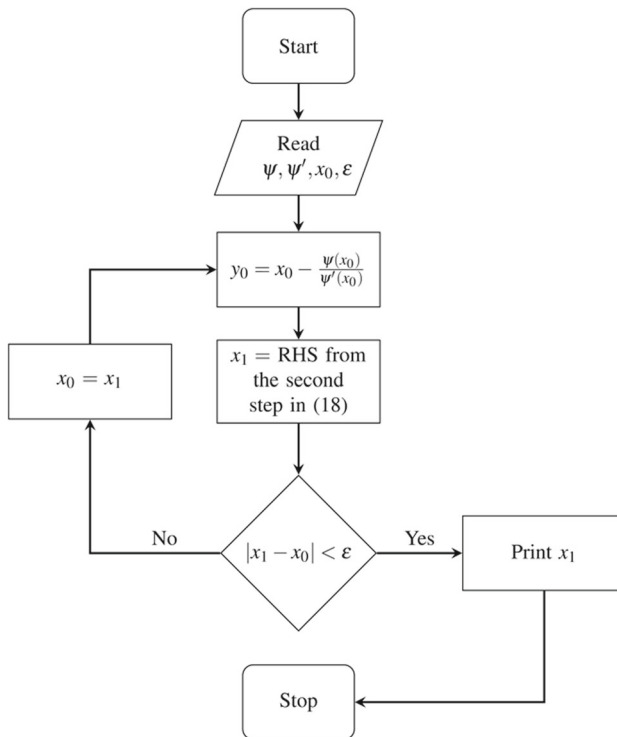

Fig. 1 Flowchart of two-step fourth-order proposed method given in (18)

using a Taylor series expansion. If the initial estimate of the root is within the radius of convergence, the iterative method is guaranteed to converge to the root. Common root-finding methods that are analyzed using local convergence analysis include Newton's method, the secant method, and the bisection method. By analyzing the behavior of these methods, it is possible to determine their strengths and weaknesses and to identify conditions under which they are most effective. Therefore, we also attempt to discuss the local convergence for (18) with the Taylor series expansion for which we need to state the following theorem.

Theorem 2 *Suppose that $\gamma \in D$ is the exact root of a differentiable function $\psi : D \subset \mathbb{R} \to \mathbb{R}$ defined for an open interval D. Then, the two-step method given in (18) has fourth-order convergence, and the asymptotic error term is as follows:*

$$e_{n+1} = -c_2(c_2^2 + c_3)e_n^4 + \mathcal{O}(e_n^5), \tag{19}$$

where $e_n = x_n - \gamma$, and $c_r = \dfrac{\psi^{(r)}(\gamma)}{r!\psi'(\gamma)}, r = 2, 3, 4, \ldots$.

Proof Expanding $\psi(x_n)$ via Taylor series expansion about γ, we obtain

$$\psi(x_n) = \psi'(\gamma)\left[e_n + c_2 e_n^2 + c_3 e_n^3 + c_4 e_n^4 + \mathcal{O}(e_n^5)\right]. \tag{20}$$

Expanding $\psi'(x_n)$ via Taylor series expansion about γ, we obtain

$$\psi'(x_n) = \psi'(\gamma)\left(1 + 2c_2 e_n + 3c_3 e_n^2 + 4c_4 e_n^3 + \mathcal{O}(e_n^4)\right). \tag{21}$$

Dividing (20) by (21), we get

$$\frac{\psi(x_n)}{\psi'(x_n)} = e_n - c_2 e_n^2 + 2(c_3 - c_2^2)e_n^3 + (7c_2 c_3 - 4c_2^3 - 3c_4)e_n^4 + \mathcal{O}(e_n^5). \tag{22}$$

Substituting (22) in the first-step of (18), we obtain

$$\hat{e} = c_2 e_n^2 + 2(c_3 - c_2^2)e_n^3 + (4c_2^3 + 3c_4 - 7c_2 c_3)e_n^4 + \mathcal{O}(e_n^5), \tag{23}$$

where $\hat{e} = y_n - \gamma$. Using the Taylor's series for $\psi(y_n)$ around γ, we obtain

$$\psi(y_n) = \psi'(\gamma)\left[e_n + c_2 \hat{e}_n^2 + c_3 \hat{e}_n^3 + c_4 \hat{e}_n^4 + \mathcal{O}(\hat{e}_n^5)\right]. \tag{24}$$

By using (23), the above expansion of $\psi(y_n)$ gives

$$\psi(y_n) = \psi'(\gamma)\left[c_2 e_n^2 + 2(c_3 - c_2^2)e_n^3 + (5c_2^3 + 3c_4 - 7c_2 c_3)e_n^4 + \mathcal{O}(e_n^5)\right]. \tag{25}$$

Now, substituting (20), (21), and (25) in the second step of (18), the error equation is obtained as

$$e_{n+1} = -c_2(c_2^2 + c_3)e_n^4 + \mathcal{O}(e_n^5). \tag{26}$$

The error equation clearly suggests that the proposed method (18) has fourth-order convergence. It is also an optimal method in the sense of Kung–Traub conjecture. □

5 Local convergence analysis: second approach

According to the proof of Theorem 2, the function ψ must be at least five times differentiable for its conclusions to be valid. Therefore, we do not know if the method (18) converges by this result if ψ is not at least five times differentiable although it may converge. Hence, the applicability of this result is limited to solving equations satisfying these constraints. Thus, many equations are left unhandled. For example,

$$\psi(x) = \begin{cases} x^3 \log x^2 + x^5 - x^4, & \text{if } x \neq 0, \\ 0, & \text{if } x = 0. \end{cases} \tag{27}$$

Since

$$\psi'''(x) = 22 - 24x + 60x^2 + 6\log x^2, \tag{28}$$

is not bounded on $[-0.5, 1.5]$. Thus, the convergence of the method (18) is not guaranteed by the analysis carried out in the earlier section. Notice also that the only derivative in (18) is ψ'. It follows that there is a need to develop a local convergence result based on the derivatives in the method (18). This is the purpose of this section. The concept of w-continuity [9] shall be used (see the new convergence conditions (H) that follow). In order to achieve this objective, let us first rewrite the method (18) in a more convenient way for our approach.

Suppose that all iterates in (18) exist for each $n = 0, 1, 2, \ldots$. Set $C_n = \psi(x_n) - 3\psi(y_n)$, $A_n = \psi'(x_n)C_n$ and $B_n = \psi(x_n)(\psi(x_n) - 2\psi(y_n)) - 2\psi(y_n)$. Then, the expression $A_n^{-1}B_n$ can be rewritten as follows:

$$A_n^{-1}B_n = \frac{\psi(x_n)(\psi(x_n) - 3\psi(y_n)) + \psi(x_n)\psi(y_n) - \psi(y_n)^2}{\psi'(x_n)(\psi(x_n) - 3\psi(y_n))},$$

$$= \frac{\psi(x_n)}{\psi'(x_n)} + \frac{\psi(y_n)(\psi(x_n) - \psi(y_n))}{\psi'(x_n)(\psi(x_n) - 3\psi(y_n))} = x_n - y_n + \frac{\psi(y_n)(\psi(x_n) - \psi(y_n))}{\psi'(x_n)(\psi(x_n) - 3\psi(y_n))}.$$

Hence, the method can be rewritten in the form

$$x_{n+1} = y_n - \psi'(x_n)^{-1}\psi(y_n) - 2\psi'(x_n)^{-1}\psi(y_n)C_n^{-1}\psi(y_n). \tag{29}$$

Notice that

$$\frac{\psi(y_n)(\psi(x_n) - \psi(y_n))}{\psi'(x_n)(\psi(x_n) - 3\psi(y_n))} = \frac{\psi(y_n)(\psi(x_n) - \psi(y_n) - 2\psi(y_n) + 2\psi(y_n))}{\psi'(x_n)(\psi(x_n) - 3\psi(y_n))}$$

$$= \psi'(x_n)^{-1}\psi(y_n) + 2\psi'(x_n)^{-1}\psi(y_n)C_n^{-1}\psi(y_n).$$

Next, some needed functions and parameters are developed. Set $M = [0, +\infty)$. Suppose that there exists a continuous and non-decreasing function $\Omega_0 : M \to \mathbb{R}$ so that the equation $\Omega_0(t) - 1 = 0$ has a smallest positive solution denoted as ρ_0. Set $M_0 = [0, \rho_0)$. The equation $g_1(t) - 1 = 0$ has a smallest solution denoted as $r_1 \in M_0 \setminus \{0\}$, where $\Omega : M_0 \to \mathbb{R}$ is a continuous and non-decreasing function and $g_1 : M_0 \to \mathbb{R}$ is a function defined by

$$g_1(t) = \frac{\int_0^1 \Omega((1-\theta)t)d\theta}{1 - \Omega_0(t)}.$$

The equation $q(t) - 1 = 0$ has a smallest solution denoted as $r_q \in M_0 \setminus \{0\}$, where $q : M_0 \to \mathbb{R}$ is defined by

$$q(t) = \frac{1}{2}\left[\int_0^1 \Omega((1-\theta)t)d\theta + 3(1 + \int_0^1 \Omega_0(\theta g_1(t)t)d\theta)g_1(t) + 1\right].$$

Set $\rho_1 = min\{\rho_0, \rho_q\}$ and $M_1 = [0, \rho_1)$. The equation $g_2(t) - 1 = 0$ has a smallest solution denoted as $r_2 \in M_1 \setminus \{0\}$, where $g_2 : M_1 \to \mathbb{R}$ is defined by

$$g_2(t) = \left[\frac{\int_0^1 \Omega(1-\theta)g_1(t)t\,d\theta}{1 - \Omega_0(g_1(t)t)} + \frac{\bar{\Omega}(t)(1 + \int_0^1 \Omega_0(\theta g_1(t)t)d\theta)}{(1 - \Omega_0(t))(1 - \Omega_0(g_1(t))t)}\right.$$
$$\left. + \frac{(1 + \int_0^1 \Omega_0(\theta g_1(t)t)d\theta)^2}{(1 - q(t))(1 - \Omega_0(t))}\right]g_2(t),$$

where

$$\bar{\Omega}(t) = \begin{cases} \Omega((1 + g_1(t))t) \\ OR \\ \Omega_0(t) + \Omega_0(g_1(t)t). \end{cases} \tag{30}$$

The smallest of the two versions used in practice.

It is proven in Theorem 3 that a possible radius of convergence for (29) is defined by the formula

$$r = \min\{r_1, r_2\}. \tag{31}$$

Set $M_2 = [0, r)$. It follows by these definitions that for each $t \in M_2$ the following estimates hold

$$0 \leq \Omega_0(t) < 1, \tag{32}$$
$$0 \leq q(t) < 1, \tag{33}$$

and

$$0 \leq g_i(t) < 1. \tag{34}$$

The notation $S[\lambda^*, a]$, $S[\lambda^*, a]$ is adopted to denote the open and closed intervals with center λ^* and of radius $a > 0$. Next, it is time to connect the functions Ω_0, Ω and the parameter r to the functions appearing in the method provided that $\lambda^* \in \Phi$

denotes a solution of the equation $\psi(x) = 0$ so that $\psi'(\lambda^*) \neq 0$ and Φ stands for a subset of the real line.

Theorem 3 *Suppose:*

(H_1) $|\psi'(\lambda^*)^{-1}(\psi'(v) - \psi'(\lambda^*))| \leq \Omega_0(|v - \lambda^*|)$ *for each $v \in \Phi$ Set $\Phi_0 = \Phi \bigcap S[\lambda^*, \rho_0]$.*

(H_2) $|\psi'(\lambda^*)^{-1}(\psi'(v_2) - \psi'(v_1))| \leq \Omega(|v_2 - v_1|)$ *for each $v_1, v_2 \in \Phi_0$*

(H_3) $S[\lambda^*, r] \in \Phi$.

The conditions (H_1)–(H_3) are called (H) for brevity. The local convergence of the method (29) is based on the developed terminology and under the conditions (H). Under conditions (H), choose the starting point $x_0 \in S(\lambda^*, r) \setminus \{\lambda^*\}$. Then, the sequence $\{x_n\}$ generated by the formula (29) converges to the solution of the equation $\psi(x) = 0$ so that for each $n = 0, 1, 2, \ldots$.

$$|y_n - \lambda^*| \leq g_1(|x_n - \lambda^*|)|x_n - \lambda^*| \leq |x_n - \lambda^*| < r \qquad (35)$$

and

$$|x_{n+1} - \lambda^*| \leq g_2(|x_n - \lambda^*|)|x_n - \lambda^*| \leq |x_n - \lambda^*|, \qquad (36)$$

where the functions g_i are defined previously and the radius r is given by the formula (31).

Proof The assertions (35) and (36) are proven using induction. Let $u \in S(\lambda^*) \setminus \{\lambda^*\}$ be an arbitrary selection. By applying the condition (H_1) and (35), we get in turn that

$$|\psi'(\lambda^*)^{-1}(\psi'(u) - \psi'(\lambda^*))| \leq \Omega_0(|u - \lambda^*|) \leq \Omega_0(r) < 1. \qquad (37)$$

Then the Banach lemma for function together with (37) give $\psi'(u) \neq 0$ and

$$|\psi'(u)^{-1}\psi'(\lambda^*)| \leq \frac{1}{1 - \Omega_0(|u - \lambda^*|)}. \qquad (38)$$

If $u = x_0$, then the iterate y_0 is well defined by the first substep of (29). We can also write

$$y_0 - \lambda^* = x_0 - \lambda^* - \psi'(x_0)\psi(x_0)$$
$$= \int_0^1 (\psi'(\lambda^* + \theta(x_0 - \lambda^*))d\theta - \psi'(x_0))(x_0 - \lambda^*),$$

leading by (H_2), (31) and (38)

$$|y_0 - \lambda^*| \leq \frac{\int_0^1 \Omega((1-\theta)|x_0 - \lambda^*|)d\theta|x_0 - \lambda^*|}{1 - \Omega_0(|x_0 - \lambda^*|)} \leq g_1(|x_0 - \lambda^*|)|x_0 - \lambda^*|$$
$$\leq |x_0 - \lambda^*| < r, \qquad (39)$$

proving that the iterates $y_0 \in S[\lambda^*, r) \setminus \{\lambda^*\}$ and additionally that the assertion (35) holds if $n = 0$. Next, in order to establish the existence of the iterate x_1, we must prove that $C_0 \neq D_0$. Notice that

$$
\begin{aligned}
C_0 - 2\psi'(\lambda^*)(x_0 - \lambda^*) &= \psi(x_0) - 3\psi(y_0) - 2\psi'(\lambda^*)(x_0 - \lambda^*) \\
&= \psi(x_0) - \psi(\lambda^*) - \psi'(\lambda^*)(x_0 - \lambda^*) - 3(\psi(y_n) - \psi(\lambda^*)) \\
&\quad - \psi'(\lambda^*)(x_0 - \lambda^*),
\end{aligned}
$$

so by (H_1) and the definition of the function q, for $x \neq \lambda^*$, we get to in turn

$$
\begin{aligned}
&|(2\psi'(\lambda^*)(x_0 - \lambda^*))^{-1}(C_0 - 2\psi'(\lambda^*))(x_0 - \lambda^*))| \\
&\leq \frac{1}{2|x_0 - \lambda^*|}\left(\int_0^1 \Omega((1-\theta)|x_0 - \lambda^*|)d\theta|x_0 - \lambda^*| \right. \\
&\quad \left. + 3(1 + \int_0^1 \Omega_0(\theta|y_n - \lambda^*|)d\theta)|y_n - \lambda^*| + |x_0 - \lambda^*|\right) \\
&\leq q_n(|x_0 - \lambda^*|) \leq q(r) < 1.
\end{aligned}
\tag{40}
$$

Thus,

$$
|C_0^{-1}\psi'(\lambda^*)| \leq \frac{1}{2(1 - q_n)},
\tag{41}
$$

so the iterate x_1 is well defined by the second substep of (29) if $n = 0$. Moreover, we can write in turn (29) that by

$$
\begin{aligned}
x_1 - \lambda^* &= y_0 - \lambda^* - \psi'(y_0)^{-1}\psi(y_0) + (\psi'(y_0)^{-1} - \psi'(x_0)^{-1})\psi(y_0) \\
&\quad - 2\psi'(x_0)^{-1}\psi(y_0)C_0^{-1}\psi(y_0),
\end{aligned}
$$

leading by the definition of the function g_2 to

$$
\begin{aligned}
|x_1 - \lambda^*| &= \left[\frac{\int_0^1 \Omega((1-\theta)|y_n - \lambda^*|)d\theta}{1 - \Omega_0(|y_n - \lambda^*|)} + \frac{\bar{\Omega}_n(1 + \int_0^1 \Omega_0(\theta|y_n - \lambda^*|)d\theta)}{(1 - \Omega_0(x_0 - \lambda^*|))(1 - \Omega_0(|y_0 - \lambda^*|))} \right. \\
&\quad \left. + \frac{2(1 + \int_0^1 \Omega_0(\theta|y_n - \lambda^*|)d\theta)}{2(1 - q_0)(1 - \Omega_0(|x_0 - \lambda^*|))}\right]|y_0 - \lambda^*| \leq g_2(|x_0 - \lambda^*|)|x_0 - \lambda^*| \\
&\leq |x_0 - \lambda^*|,
\end{aligned}
\tag{42}
$$

where we also used (39) and

$$
\Omega_n^1 = \begin{cases} \Omega(|x_n - \lambda^*| + |y_n - \lambda^*|), \\ \Omega_0(|x_n - \lambda^*| + \Omega_0(|y_n - \lambda^*|), \end{cases}
\tag{43}
$$

and

$$
\psi(y_0) = \psi(y_0) - \psi(\lambda^*) = \int_0^1 \psi'(\lambda^* + \theta(y_0 - \lambda^*))d\theta(y_0 - \lambda^*)(y_n - \lambda^*),
$$

so

$$|\psi'(\lambda^*)^{-1}\psi(y_0)| \le (1 + \int_0^1 \Omega_0(\theta|y_0 - \lambda^*)d\theta)|y_0 - \lambda^*|.$$

Thus, it follows by (43) that the iterate $x_1 \in S[\lambda^*, r] \setminus \{\lambda^*\}$ and the assertion (37) holds if $n = 0$. Then, S with x_0, y_0, x_1 by x_m, y_m, x_{m+1} in the preceding calculations to complete the induction for the assertions (36) and (37). Finally, from the estimation

$$|x_{m+1} - \lambda^*| \le d|x_m - \lambda^*| < r,$$

where $d = g_1(|x_0 - \lambda^*|) \in [0, 1)$, we concluded that $\lim_{m\to\infty} x_m = \lambda^*$ and $\{x_m\} \subset S[\lambda^*, r]$. □

The uniqueness interval for the solution λ^* is determined in the next result.

Proposition 1 *Suppose that there exists a solution* $y^* \in S(\lambda^*, \rho_2)$ *of the equation* $\psi(x) = 0$ *for some* $\rho_2 > 0$, *the condition* (H_2) *holds in the interval* $S(\lambda^*, \rho_2)$, *and for some* $\rho_3 \ge \rho_2$

$$\int_0^1 \Omega_0(\theta\rho_3)d\theta < 1. \tag{44}$$

Set $\Phi_1 = \Phi \bigcap S[\lambda^*, \rho_3]$. *Then, the only solution of the equation* $\psi(x) = 0$ *in the domain* Φ_1 *is* λ^*.

Proof Let $y^* \in \Phi_1$ be such that $\psi(y^*) = 0$. Define the function $T = \int_0^1 \psi'(\lambda^* + \theta(y^* - \lambda^*))d\theta$. It follows by (H_1) and (44) in turn that

$$|\psi'(\lambda^*)^{-1}(T - \psi'(\lambda^*))| \le \int_0^1 \Omega_0(\theta|y^* - \lambda^*|)d\theta \le \int_0^1 \Omega_0(\theta\rho_3)d\theta < 1,$$

thus $T \ne 0$ and $y^* - \lambda^* = T^{-1}(\psi(y^*) - \psi(\lambda^*)) = T^{-1}(0) = 0$. Hence, we deduce that $y^* = \lambda^*$ □

Remark 1 If all the (H) conditions hold, then we can set $\rho_2 = r$.

6 Semilocal convergence

This type of analysis requires the concept of majorizing sequences [4, 5]. Let us define for $t_0 = 0$, $s_0 \ge 0$ and each $n = 0, 1, 2, \ldots$. Consider

$$\bar{q}_n = \frac{3\int_0^1 \Omega_0((1-\theta)(s_n - t_n))d\theta}{1 - \Omega(t_n)}.$$

Then, the sequence $\{t_n\}$ is given by

$$t_{n+1} = s_n + \left[\frac{\int_0^1 \Omega((1-\theta)(s_n - t_n))d\theta}{1 - \Omega_0(t_n)} + \frac{2\left(\int_0^1 \Omega((1-\theta)(s_n - t_n))d\theta \right)^2}{(1-\bar{q}_n)(1-\Omega_0(t_n))^2} \right](s_n, t_n),$$

$$\Pi_{n+1} = \int_0^1 \Omega((1 - \theta)(t_{n+1} - t_n))d\theta(t_{n+1} - t_n) + (1 + \Omega_0(t_n))(t_{n+1} - s_n),$$

$$s_{n+1} = t_{n+1} + \frac{\Pi_{n+1}}{1 - \Omega_0(t_{n+1})}. \tag{45}$$

Under certain conditions, the sequence $\{t_n\}$ is shown to be majorizing for the method (29) in Theorem 4. But let us first provide convergence conditions for it.

Lemma 1 *Suppose that there exists $A > 0$ such that for each $n = 0, 1, 2, \ldots$*

$$\Omega_0(t_n) < 1, \quad \bar{q}_n < 1, \quad and \quad t_n < \mu. \tag{46}$$

Then the following assertion hold

$$0 \le t_n \le s_n \le t_{n+1} \le t^* \le \mu \tag{47}$$

and

$$\lim_{n \to \infty} t_n = t^*. \tag{48}$$

Proof The assertion (47) and (48) follow immediately by the conditions (46) and the definition of the sequence $\{t_n\}$ given by the formula (6). □

Remark 2 If we suppose that the equation $\Omega_0(t) - 1 = 0$ has a smallest positive solution μ_0, then we can take $\mu = \mu_0$. Next, as in the local case, we connect the sequence $\{t_n\}$ and the functions in the method (29) provided that there exists $x_0 \in \Phi$ such that $\psi'(x_0) \ne 0$. Suppose:

(h_0) $|\psi'(x_0)^{-1}\psi(x_0)| \le s_0$.
(h_1) $|\psi'(x_0)^{-1}(\psi'(v) - \psi'(x_0))| \le \Omega_0(|v - x_0|)$ for each $v \in \Phi$.
Set $\Phi_2 = \Phi \bigcap S(x_0, \mu_0)$.
(h_2) $|\psi'(x_0)^{-1}(\psi'(v_2) - \psi'(v_1))| \le \Omega(|v_2 - v_1|)$ for each $v_1, v_2 \in \Phi_2$.
(h_3) The condition (46) holds.
and
(h_4) $S[x_0, t^*] \subset \Phi$.
We shall refer to (h_0)–(h_4) as the conditions (h).
Then, we prove the semilocal convergence of the method (29).

Theorem 4 *Suppose that the conditions (h) hold. Then, the following assertions hold*

$$\{y_k\}, \{x_k\} \subset S[x_0, t^*) \tag{49}$$

$$|y_k - x_k| \le s_k - t_k \tag{50}$$

$$|x_{k+1} - y_k| \le t_{k+1} - s_k \tag{51}$$

and there exists $\lambda^* \in S[x_0, t^*]$ solving the equation $\psi(x) = 0$.

Proof These time similar calculations are carried out to the local case out using x_0, (h) for λ^*, (H). First, notice that by the condition (h_0),

$$|y_0 - x_0| = |\psi'(x_0)^{-1}\psi(x_0)| \le s_0 = s_0 - t_0 < t^*.$$

Thus the iterate $y_0 \in S[x_0, t^*)$ and (50) holds if $k = 0$. We can write

$$
\begin{aligned}
C_k - \psi'(x_0)(y_0 - x_0) &= \psi(x_k) - 3\psi(y_k) - \psi'(x_0)(y_k - x_k) \\
&= \psi(x_k) - \psi(y_k) - \psi'(x_k)(x_k - y_k) + \psi'(x_k)(x_k - y_k) \\
&\quad - 2\psi(y_k) - \psi'(x_0)(y_k - x_k).
\end{aligned} \tag{52}
$$

$$
\begin{aligned}
C_k + \psi'(x_k)(y_k - x_k) &= \psi(x_k) - 3\psi(y_k) + \psi'(x_k)(y_k - x_k) \\
&= \Big[\psi(y_k) - \psi(x_k) - \psi'(x_k)(y_k - x_k)\Big] - 2\psi(y_k).
\end{aligned}
$$

But

$$\psi(y_k) = \psi(y_k) - \psi(x_k) - \psi'(x_k)(y_k - x_k),$$

thus

$$C_k + \psi'(x_k)(y_k - x_k) = -3\int_0^1 \Big[\psi'(x_k + \theta(y_k - x_k))d\theta - \psi'(x_k)\Big](y_k - x_k).$$

Consequently, we have

$$|\psi'(x_0)^{-1}(C_n + \psi'(x_k)(y_k - x_k))| \le 3\int_0^1 \Omega(\theta|y_k - x_k|)d\theta|y_k - x_k|.$$

Then, it follows for $y_k \ne x_k$

$$
\begin{aligned}
&|(-\psi'(x_k)(y_k - x_k))^{-1}(C_k + \psi'(x_k)(y_k - x_k))| \\
&\le 3|\psi'(x_k)^{-1}\psi'(x_0)(|y_0 - x_k|)^{-1}\int_0^1 \Omega(1 - \theta)|y_k - x_k|)d\theta|y_k - x_k| \\
&\le \frac{3\int_0^1 \Omega((1 - \theta)(s_k - t_k))d\theta}{1 - \Omega_0(t_k)} = \bar{q}_n < 1.
\end{aligned} \tag{53}
$$

So

$$|C_k^{-1}\psi(x_0)| \le \frac{1}{(1 - \bar{q}_k)(1 - \Omega_0(t_k))|y_k - x_k|}. \tag{54}$$

Hence, the iterate x_{k+1} is well defined and

$$
\begin{aligned}
|x_{k+1} - y_k| &\leq |\psi'(x_k)^{-1}\psi'(x_0)||\psi'(x_0)^{-1}\psi(y_k)| \\
&\quad + 2|\psi(x_k)^{-1}\psi'(x_0)||C_k^{-1}\psi'(x_0)|(|\psi'(x_0)^{-1}\psi(y_k)|)^2 \\
&\leq \left[\frac{(\int_0^1 \Omega(1-\theta)(s_k-t_k))d\theta}{1-\Omega_0(t_k)} + \frac{2(\int_0^1 \Omega(1-\theta)(s_k - t_k))d\theta)^2}{(1 - \omega_0(t_k))^2(1 - \bar{q}_k)} \right](s_k - t_k) \\
&= t_{k+1} - s_k,
\end{aligned}
\tag{55}
$$

thus

$$
|x_{k+1} - x_0| \leq |x_{k+1} - y_k| + |y_k - x_0| \leq t_{n+1} - s_n + s_n - t_0 = t_{n+1} < t^*.
$$

It follows that the iterates $x_{n+1} \in S[x_0, t^*)$ and the assertion (51) holds. Moreover, the first substep of (29) gives

$$
\begin{aligned}
\psi(x_{k+1}) &= \psi(x_{k+1}) - \psi(x_k) + \psi(x_k) = \psi(x_{k+1}) - \psi(x_k) - \psi'(x_k)(y_k - x_k) \\
&= \psi(x_{k+1}) - \psi(x_k) - \psi'(x_k)(x_{k+1} - x_k) + \psi(x_k)(x_{k+1} - x_k) \\
&\quad -\psi'(x_k)(y_k - x_k).
\end{aligned}
$$

Hence,

$$
|\psi'(x_0)^{-1}\psi(x_{n+1})| \leq \int_0^1 \Omega((1-\theta)|x_{k+1}-x_k|)d\theta|x_{n+1} - x_n| + (1 + \Omega(t_k))(t_{k+1} - s_k)
$$
$$
= \Pi_{n+1}.
\tag{56}
$$

Furthermore, we obtain

$$
|y_{k+1}-x_{k+1}| \leq |\psi'(x_{k+1})^{-1}\psi'(x_0)||\psi'(x_0)^{-1}\psi(x_{k+1})| \leq \frac{\Pi_{k+1}}{1 - \omega_0(t_{k+1})} = s_{k+1} - t_{k+1}
$$

and

$$
|y_{k+1} - x_0| \leq |y_{k+1} - x_{k+1}| + |x_{k+1} - x_0| \leq s_{k+1} - t_{k+1} + t_{k+1} - t_0 = s_{k+1} < t^*.
$$

Therefore, the induction for the assertions (49)–(51) is completed. In new of the fact that $\{t_k\}$ is fundamental (as convergent), the sequence $\{x_k\}$ is also fundamental. Hence, there exists $\lambda^* \in S[x_0, t^*]$ such that $\lim_{k \to \infty} x_k = \lambda^*$. Finally, by letting $n \to \infty$ in (56) using the continuity of ψ, we concluded $\psi(\lambda^*) = 0$. ☐

The uniqueness of the solution is determined as in the local convergence case.

Proposition 2 *Suppose:*
The equation $\psi(x) = 0$ has a solution $y^* \in S(x_0, \rho_4)$ for some $\rho_4 > 0$.

The condition (h_1) holds on the interval $S[x_0, \rho_4)$ and there exists $\rho_5 \geq \rho_4$ such that

$$\int_0^1 \Omega((1-\theta)\rho_4 + \theta\rho_5)d\theta < 1. \tag{57}$$

Set $\Phi_3 = \Phi \bigcup S[x_0, \rho_5]$.
Then, the equation $\psi(x) = 0$ is uniquely solvable by y^*.

Proof Let $z^* \in \Phi_3$ with $\psi(z^*) = 0$. Define the function $T_1 = \int_0^1 \psi'(y^* + \theta(z^* - y^*))d\theta$. Then, by (57), we obtain in turn

$$|\psi'(x_0)^{-1} < T_1 - \psi('(x_0)| \leq \int_0^1 (1-\theta)|y^* - x_0| + \theta|z^* - x_0|)d\theta$$
$$\leq \int_0^1 \Omega_0(1-\theta)\rho_4 + \theta\rho_5)d\theta < 1,$$

thus $z^* = y^*$. □

Proposition 3 *If the limit point t^* in the conditions (h_0)–(h_4) holds, then set by $y^* = \lambda^*$ and $\rho_4 = t^*$ in the Proposition 2.*

7 Numerical and graphical results

In this section, we present some numerical and graphical results obtained with the proposed method. Numerical experiments are divided into two groups, that is, into academic examples and real-life applications. The graphical examples consists of polynomiographs generated for several complex polynomials. In each case, we compare the proposed method (PONM – (18)) with other fourth-order methods known in the literature (KJNM – (3), OWNM – (4), OZNM –(5), KTNM – (6)).

7.1 Polynomiography

Polynomiography—a term introduced by Kalantari around 2000—plays an important role in the modern analysis of the quality of the root-finding methods [20]. The methods of polynomiography (basins of attraction, dynamics planes, speed of convergence etc.) were present in the literature much earlier, but Kalantari was the first who gave them a common name. Kalantari defined it as the art and science of visualizing the approximation of the zeros of complex polynomials using iteration functions [12] and called the image obtained by polynomiography a polynomiograph. In this subsection, we present polynomiographs and numerical measures computed from them for three different polynomials and compare the obtained results for the proposed method with some other fourth-order methods from the literature.

The general method for generating polynomiographs is presented in Algorithm 1. There are several methods of determining the color in the algorithm. We selected a method that combines the basins of attraction and the speed of convergence of the

given root-finding method into one polynomiograph [2]. In the method, each root of the polynomial ψ gets a distinct color, and, additionally, we set a black color for non-convergent points. Then, for each point z_0 in the considered area A, we iterate the given root-finding method R using the maximum of N iterations. After finishing the iteration process, if we performed less than N iterations (the method has converged to a root), then we search for the root closest to z_{n+1} and take its color. Basing on the number of performed iterations, we set the shade of the color (dark, high number of iterations; light, low number of iterations), and color z_0 using this color. In the case where the root-finding method has not converged to any root (we performed the maximum of N iterations), we color z_0 using the black color. Using such a coloring method, the color of the point gives us information on the root to which the starting point has converged, and the shade of the color gives us information on the speed of convergence.

Algorithm 1: Generation of a polynomiograph.

Input	: $\psi \in \mathbb{C}[Z]$, deg $\psi \geq 2$ – polynomial; R – root finding method; $A \subset \mathbb{C}$ – area; N – the maximum number of iterations; ε – accuracy.
Output	: Polynomiograph for the complex-valued polynomial ψ within the area A.

1 **for** $z_0 \in A$ **do**
2 $\quad$ $n = 0$
3 $\quad$ **while** $n \leq N$ **do**
4 $\quad\quad$ $z_{n+1} = R(z_n, \psi)$
5 $\quad\quad$ **if** $|z_{n+1} - z_n| < \varepsilon$ **then**
6 $\quad\quad\quad$ break
7 $\quad\quad$ $n = n + 1$
8 $\quad$ Determine the color for z_0 based on z_n and n.

Polynomiographs are used to visually analyze and compare root-finding methods. But, we can compute some numerical measures based on a polynomiographs which will allow a better analysis of the methods. In the literature, there are three such measures: average number of iterations (ANI) [3], convergence area index (CAI) [3], and generation time [8]. The average number of iterations is computed by averaging the number of performed iterations (which is coded as the shade of the color in the polynomiograph) for all points in the polynomiograph. CAI is computed as the ratio of the number of starting points that converged to any root (points other than black in the polynomiograph) to the number of all points in the polynomiograph. From the definition of CAI, we see that its value is between 0 and 1, and it gives us information about the percentage of the area shown in the polynomiograph that has converged to roots. The generation time gives us information about the real time of computations because it is the time needed to generate the polynomiograph.

In this section, we generated polynomiographs for three complex polynomials:

- $\psi_2(z) = z^2 - 1$, roots: $-1, 1$.
- $\psi_3(z) = z^3 - 1$, roots: $1, -\frac{1}{2} + \frac{\sqrt{3}}{2}i, -\frac{1}{2} - \frac{\sqrt{3}}{2}i$.
- $\psi_4(z) = z^4 - 0.75z^2 - 0.25$, roots: $-1, 1, -0.5i, 0.5i$.

For each of the polynomials ψ_2, ψ_3, ψ_4, the other parameters used to generate poly-nomiographs were the following: $A = [-2, 2]^2$, $N = 30$, $\varepsilon = 0.001$, image resolution of 1000×1000 pixels. The experiments were performed on the computer with the following specifications: Intel i5-9600K (@3.70 GHz), 32 GB DDR4 RAM, and Windows 10 (64 bit). The program for generating polynomiographs was implemented in Mathematica 13.2 using the parallelization option of the SPSVERBc1 command.

The polynomiographs for the ψ_2 polynomial generated using various root-finding methods are presented in Fig. 2, and the numerical measures calculated from them in Table 1. From the polynomiographs, we see that the best stability in finding the roots have the OWNM and OZNM methods. The plane is divided into two equal basins, so that for the starting points for which the real part is less than zero, converge to -1, and the points from the other half of the plane to 1. For the other methods, the stability is lost in the neighborhood of the vertical line passing through the origin. We see that the two basins are intertwined. The smallest interweaving is visible for the PONM method. The speed of convergence is very similar for all methods, i.e., small differences in the shades of the colors. This is confirmed by the values of ANI in Table 1. The values are between 2.341 and 3.016, where the lowest value was obtained using the PONM method. The generation times are also very similar for all the methods. They vary between 0.692 and 0.706 s, where the shortest time was obtained by the OZNM method. For the CAI measure, we see that for all the methods considered, each starting point in A has converged to a root, i.e., a CAI value equal to 1.0.
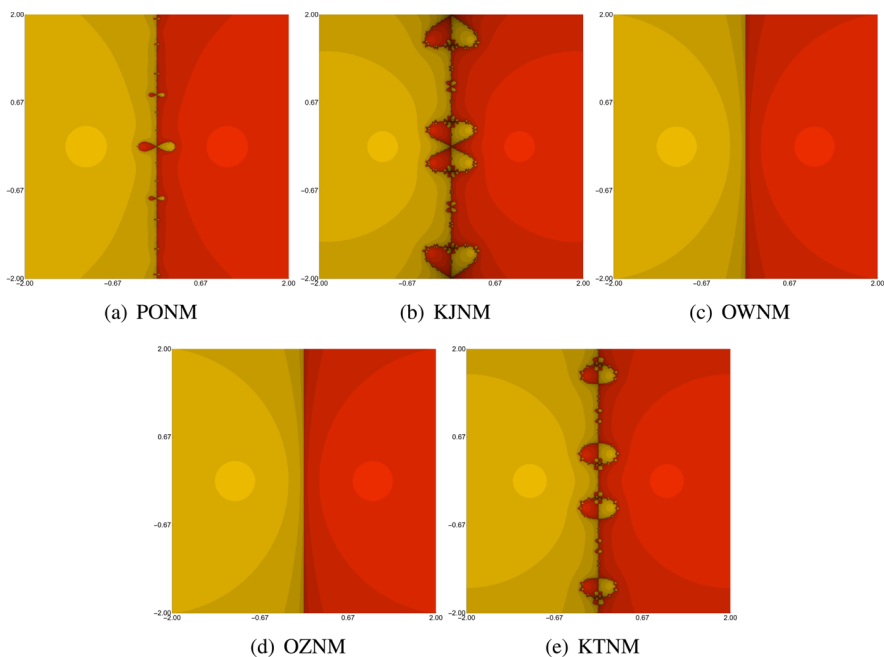

Fig. 2 Polynomiographs for the complex polynomial ψ_2 generated using various root-finding methods

Table 1 Numerical measures obtained from the polynomiographs generated for ψ_2 (Fig. 2)

Method	ANI	CAI	Time (s)
PONM	2.341	1.0	0.705
KJNM	3.016	1.0	0.706
OWNM	2.380	1.0	0.694
OZNM	2.380	1.0	0.692
KTNM	2.755	1.0	0.702

The resulting polynomiographs and the values of numerical measures obtained for the ψ_3 polynomial are gathered in Fig. 3 and Table 2, respectively. In this case, we see a diverse behavior of the methods. In each case, we can observe characteristic braids, but their shape differs for each method. The interweaving of the basins around the braids is the smallest for the OWNM and OZNM methods, and the braids are similar. For the other three methods, the braids form various shapes and have different complexities. The most complex braids are visible for the PONM method, and the interweaving of the basins is the biggest. The behavior of the methods outside the braids is very similar, that is, the methods converge to the same roots and have a similar speed of convergence. When we look at the values of the numerical measures collected in Table 2, we see that the lowest ANI value was obtained by the OWNM method (2.863) and the highest by the KJNM method (4.632). In terms of CAI value, the best two methods were OWNM and OZNM, which obtained convergence of all
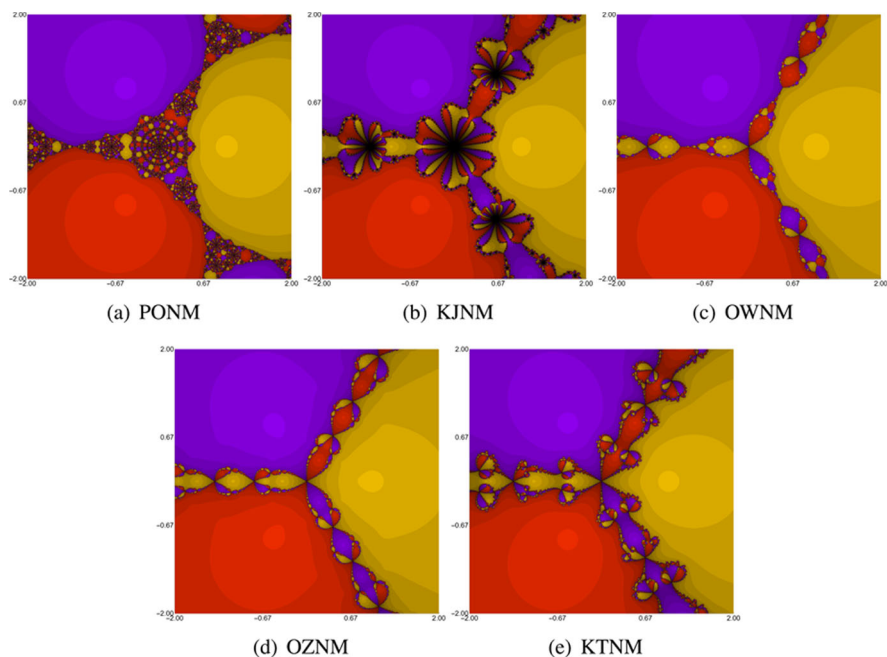

(a) PONM   (b) KJNM   (c) OWNM

(d) OZNM   (e) KTNM

Fig. 3 Polynomiographs for the complex polynomial ψ_3 generated using various root-finding methods

Table 2 Numerical measures obtained from the polynomiographs generated for ψ_3 (Fig. 3)

Method	ANI	CAI	Time (s)
PONM	3.708	0.999	0.827
KJNM	4.632	0.996	0.828
OWNM	2.863	1.0	0.763
OZNM	3.143	1.0	0.735
KTNM	3.736	0.999	0.799

starting points in A, i.e., CAI value equal to 1.0. For the other three methods, we see that a small percentage of the starting points did not converge to any of the roots. This is clearly visible in the polynomiograph for the KJNM method (Fig. 3b), where we see black areas. When it comes to generation times, the shortest time was obtained using the OZNM method (0.735 s). But the difference between the times for the considered methods was small because the times vary between 0.735 and 0.828 s.

In the case of the last polynomial, ψ_4, the polynomiographs generated using the considered methods are presented in Fig. 4, and the values of numerical measures are collected in Table 3. This time, we see the biggest differences between the polynomiographs. The most stable behavior is visible for the OWNM method—the braids and the interweaving of the basins are smaller than for the other methods. The worst stability can be observed for the PONM method, where we do not see the characteristic braids as for the other methods. Instead, we see a large number of interweaving basins
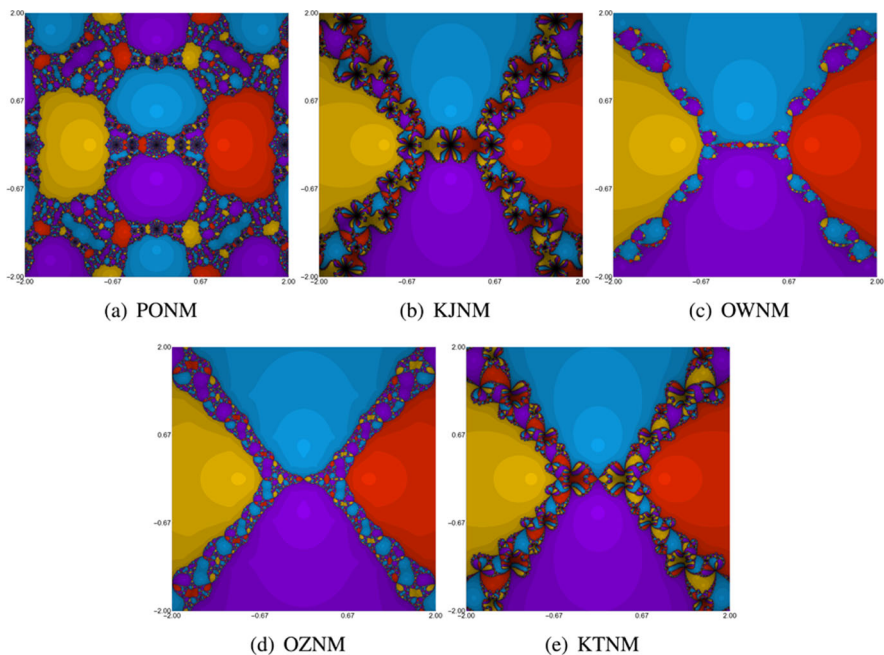

(a) PONM   (b) KJNM   (c) OWNM

(d) OZNM   (e) KTNM

Fig. 4 Polynomiographs for the complex polynomial ψ_4 generated using various root-finding methods

Table 3 Numerical measures obtained from the polynomiographs generated for ψ_4 (Fig. 4)

Method	ANI	CAI	Time (s)
PONM	5.560	0.999	0.967
KJNM	5.785	0.996	0.915
OWNM	3.498	1.0	0.844
OZNM	4.070	0.999	0.856
KTNM	4.874	0.999	0.872

resulting in a division of the basins into many small areas, forming a very interesting pattern. The speed of convergence is very similar for the OWNM, OZNM, and KTNM methods. This is confirmed by the values of ANI in Table 3, where the lowest value of ANI was obtained by the OWNM, and it is equal to 3.498. The worst speed of convergence is observed, like for the previous two polynomials, for the KJNM method (5.785). Despite the worst stability, the PONM method obtained a good convergence ratio, that is, CAI value equal to 0.999. Only the OWNM method has a higher value of CAI (1.0). When we compare the generation times, we notice that the differences are minor. The times are between 0.844 (for the OWNM method) and 0.967 s (for the PONM method).

7.2 Academic numerical experiments

In this subsection, we will use numerical simulations for some academic-type non-linear equations to demonstrate the efficacy of the proposed optimal iterative method with fourth-order convergence, as shown in (18). Many different classes of non-linear functions are considered as shown in Table 4 which contains the test function ψ, the initial guess x_0 for the method, and the exact root γ for the test function. To determine when to end the iteration process, we use the stopping criterion $|\psi(x_N)| \leq \varepsilon$, where the tolerance is set to $\varepsilon = 10^{-300}$ and the desired degree of precision is determined to be as high as 4, 000. The amount of CPU time consumed by each approach is computed in seconds. Numerical experiments were performed on a laptop with Windows 11 (64 bit), 24 GB of RAM, and Intel Core i7-1065G7 CPU (@1.50 GHz) processor.

For the numerical simulations, the following notations were used:

– TFE: Total number of function evaluations.
– N: Total number of iterations.

Table 4 Some academic test problems for the comparative analysis

Test function	Initial guess	Exact root
$\psi_1(x) = \sin(x) + \cos(x) + x$	1.5	-0.45662470456763082444
$\psi_2(x) = \cos(x) - x$	2.5	0.73908513321516064166
$\psi_3(x) = \log(x^2 + \exp(x))$	1.7	0
$\psi_4(x) = \sin(x)^2 - x^2 + 1$	6.5	1.40449164821534122260

– CPU: Computational time in seconds.

For the test functions from Table 4, we have attempted to compute the absolute error at the last iteration given as $|x_n - x_{n-1}|$, the test function's value at the last iteration given as $|\psi(x_n)|$, and the computational time in seconds. The results for the test functions $\psi_1-\psi_4$ are presented in Table 5.

It can be observed in Table 5 for the test function $\psi_1(x)$ that the only methods that could converge to the exact solution, in seven iterations, are the optimal proposed method and the method KJNM while the former is the method with the smallest absolute error and the functional value nearly equal to 0. In six iterations, the optimal proposed method yielded the smallest absolute error and thereby the smallest absolute functional value for the second test function ψ_2 as shown in Table 5. Similar results are witnessed for the remaining two test functions in Table 5 wherein the method OZNM diverges to some other solution for the test function $\psi_3(x)$.

7.3 Some real-life applications

Non-linear transcendental equations have a wide range of applications from mathematical modeling to physics, engineering, and economics. For example, in economics, these equations are used to solve problems related to demand and supply, taxation, elasticity, pricing, etc. In mathematics, these equations are used to solve non-linear differential equations and to study the stability of dynamical systems. In physics, these equations are used to describe physical phenomena such as wave motion and electrical circuits. In engineering, these equations are used to model complex systems such as aircraft and spacecraft. Moreover, they can be used to solve optimization problems

Table 5 Numerical comparison of (18) with some existing optimal methods for the test functions $\psi_1(x) - \psi_4(x)$

Method	$|x_n - x_{n-1}|$	$|\psi(x_n)|$	Time (s)	$|x_n - x_{n-1}|$	$|\psi(x_n)|$	Time (s)
	$\psi_1(x)$: $N = 7$ and $TFE = 21$			$\psi_2(x)$: $N = 6$ and $TFE = 18$		
PONM	9.37e−545	1.51e−2178	1.71e−01	1.54e−522	3.77e−2090	1.25e−01
KJNM	3.28e−49	3.30e−196	2.81e−02	4.21e−385	2.47e−1539	9.30e−02
OWNM	Failed	–	–	1.09e−421	6.02e−1686	1.87e−01
OZNM	Diverge	–	–	1.08e−84	7.08e−254	1.41e−01
KTNM	Failed	–	–	3.20e−402	6.41e−1608	9.40e−02
	$\psi_3(x)$: $N = 7$ and $TFE = 21$			$\psi_4(x)$: $N = 6$ and $TFE = 18$		
PONM	9.49e−1458	4.00e−4000	1.40e−01	1.26e−686	3.44e−2744	2.03e−01
KJNM	9.75e−421	3.62e−1680	4.70e−02	2.82e−98	2.16e−390	1.41e−01
OWNM	5.40e−604	1.69e−2413	6.20e−02	2.94e−149	7.62e−595	1.10e−01
OZNM	Diverge	–	–	8.00e−111	5.57e−332	2.50e−01
KTNM	5.55e−507	2.85e−2025	4.70e−02	1.20e−113	4.62e−452	1.25e−01

and to calculate the optimal parameters of a system. Other applications include the following:

- Engineering: non-linear systems analysis, control systems design.
- Physics: mechanics, electromagnetism, fluid dynamics, quantum mechanics.
- Biology: modeling population dynamics, spread of diseases.
- Economics: macroeconomic modeling, financial forecasting.
- Cryptography: mathematical encryption and decryption of information.
- Geology: modeling of geological systems and processes.
- Meteorology: weather forecasting, atmospheric modeling.

Problem 1 Volume from Van der Waals' equation [27].

Van der Waals equation is a mathematical expression used to describe the behavior of real gases, which deviate from the ideal gas law. The ideal gas law assumes that gas molecules have no volume and do not interact with one another, but in reality, gas molecules do have a finite volume and interact with each other through forces like attraction and repulsion. The Van der Waals equation is given as follows:

$$P = \frac{nRT}{V - nb} - \frac{an^2}{V^2}, \tag{58}$$

where:

- P is the absolute pressure of the gas.
- n is the number of moles of gas.
- R is the gas constant (0.0820578).
- T is the temperature.
- V is the volume of the gas.
- a and b are constants representing the attractive and repulsive forces between gas molecules, respectively.

The Van der Waals equation takes into account the intermolecular forces and the finite volume of gas molecules, making it a more accurate representation of real gases compared to the ideal gas law. The equation is used to predict the behavior of gases under various conditions such as pressure, temperature, and volume. It also plays a crucial role in understanding the behavior of real gases in applications like refrigeration, gas storage, and transportation. The Van der Waals equation is used in many other fields study, such as thermodynamics, chemistry, engineering, and physics. It is useful in calculating the properties of real gases such as density, enthalpy, entropy, and internal energy. It is also used to study the phase transitions of a gas and to calculate its critical point. Furthermore, it is used to model the behavior of a gas in a variety of situations, such as when a gas is subjected to shock waves or when a gas is in a closed container. (58) can be rewritten as follows:

$$(P + \frac{an^2}{V^2})(V - bn) = nRT. \tag{59}$$

The model (59) is a modified version of the ideal gas equation $V = RT/nP$. The above equation can be rearranged as follows:

$$\psi_1(V) = PV^3 - n(RT + bP)V^2 + n^2 aV - n^3 ab.$$

Substituting $P = 40$atm, $T = 773°C$, $n = 1.4$, $a = 18$ and $b = 0.1154$, we get

$$\psi_1(V) = 40V^3 - 95.26535116V^2 + 35.28V - 5.6998368. \tag{60}$$

The approximate solution for the above model up to 20 dp is given as follows:

$$V^* = 1.97078421940702941145.$$

The numerical results for the model (60) are shown in Table 6, wherein the optimal proposed method having fourth-order convergence, in eight iterations, surpasses other methods chosen for comparison irrespective of the initial guess.

Problem 2 Fluid permeability in biogels [23].

Fluid permeability in biogels refers to the ability of fluid to pass through the gel network structure. Biogels are three-dimensional hydrogel networks made up of biopolymers such as proteins, polysaccharides, or nucleic acids. The fluid permeability of a biogel is dependent on several factors, including the composition, structure, and mechanical properties of the gel. The gel's permeability is important in a number of applications. By understanding the factors that affect fluid permeability in biogels, it may be possible to design more effective and efficient biogels for a variety of applications.

Non-linear fluid permeability in biogels can be mathematically described using non-linear equations that capture the complex behavior of fluid transport through the gel network. One such equation is the Darcy's law for non-linear porous media, which accounts for the non-linear relationship between the fluid flow rate and the applied pressure difference. The equation includes terms that describe the effects of gel pore size, pore connectivity, and other factors that affect fluid permeation, and is given by

$$R_f m^3 - 20p(1 - m)^2 = 0, \tag{61}$$

Table 6 Comparison of optimal fourth-order method for Problem 1 taking $N = 8$ iterations and $TFE = 24$

Method	$V_0 = 0.5$			$V_0 = 18.5$		
	$\|V_n - V_{n-1}\|$	$\|\psi(V_n)\|$	Time (s)	$\|V_n - V_{n-1}\|$	$\|\psi(V_n)\|$	Time (s)
PONM	1.80e−932	2.32e−3725	1.40e−01	7.70e−628	7.84e−2507	4.70e−02
KJNM	4.11e−92	1.40e−363	9.40e−02	3.83e−45	1.05e−175	4.70e−02
OWNM	–	Diverge	–	1.47e−126	6.18e−502	3.10e−02
OZNM	–	Diverge	–	8.58e−43	1.26e−125	3.10e−02
KTNM	4.61e−302	1.40e−1203	4.60e−02	1.11e−62	4.73e−246	4.70e−02

where R_f stands for the radius of the fiber, p shows the specific hydraulic permeability, and $m \in [0, 1]$ is the porosity of the medium. If we assume $R_f = 100 \times 10^{-9}$ and $p = 0.4655$, we obtain the following third-degree polynomial:

$$\psi_2(m) = 1 \times 10^{-7}m^3 - 9.31m^2 + 18.62m - 9.31. \tag{62}$$

The approximate solution for the above model up to 20 dp is given as follows:

$$m^* = 1.0001036555789320136$$

The numerical results for the model (62) are shown in Table 7, wherein the optimal proposed method having fourth-order convergence, in eleven iterations, surpasses other methods chosen for comparison irrespective of the initial guess. For this cubic model, the proposed method has considerably shorter computational time in comparison to other methods in most cases.

Problem 3 Fraction conversion of nitrogen and hydrogen to ammonia [24].

The fractional conversion of nitrogen and hydrogen to ammonia refers to the percentage of the reactants that have been converted into ammonia during the reaction process. The fractional conversion is a measure of the extent of the reaction and can be used to determine optimal conditions for maximum yield. The fractional conversion is calculated as the ratio of the amount of ammonia produced to the total amount of nitrogen and hydrogen fed into the reaction system. The equation for the fractional conversion of nitrogen and hydrogen to ammonia is given by the following:

Fractional conversion = (Amount of ammonia produced)/(Total amount of nitrogen and hydrogen fed into the reaction system)

This relation provides a ratio that represents the extent to which nitrogen and hydrogen have been converted into ammonia (A). The fractional conversion can be used to monitor the progress of the reaction and determine when the reaction has reached completion. The fractional conversion is usually expressed as a decimal or a percentage. In this problem, the values of temperature and pressure have been taken as $500°C$ and 250 atm, respectively. This problem has the following non-linear form:

$$\psi_3(A) = -0.186 - \frac{8A^2(A-4)^2}{9(A-2)^3}, \tag{63}$$

Table 7 Comparison of optimal fourth-order method for Problem 2 taking $N = 11$ iterations and $TFE = 33$

Method	$\|m_n - m_{n-1}\|$ $m_0 = 3.9$	$\|\psi_2(m_n)\|$	Time (s)	$\|m_n - m_{n-1}\|$ $m_0 = 7.5$	$\|\psi_2(m_n)\|$	Time (s)
PONM	2.31e−1152	3.00e−3999	9.30e−02	9.69e−568	1.91e−2260	9.40e−02
KJNM	2.77e−12	3.85e−38	9.40e−02	1.12e−07	1.01e−19	1.09e−01
OWNM	5.85e−37	2.54e−137	9.40e−02	6.23e−19	3.27e−65	1.41e−01
OZNM	5.85e−37	1.00e−116	9.40e−02	6.23e−19	1.21e−62	6.30e−02
KTNM	3.34e−17	5.39e−58	9.40e−02	8.24e−10	2.00e−28	9.40e−02

Table 8 Comparison of optimal fourth-order method for Problem 3 taking $N = 6$ iterations and $TFE = 18$

Method	$\frac{\|A_n - A_{n-1}\|}{A_0 = 0.15}$	$\|\psi(A_n)\|$	Time (s)	$\frac{\|A_n - A_{n-1}\|}{A_0 = 0.8}$	$\|\psi(A_n)\|$	Time (s)
PONM	2.68e−865	8.90e−3459	6.20e−02	8.15e−620	7.60e−2477	6.30e−02
KJNM	4.12e−582	8.96e−2325	4.60e−02	2.04e−487	5.38e−1946	3.10e−02
OWNM	4.58e−743	6.46e−2969	3.10e−02	4.98e−523	9.00e−2089	3.20e−02
OZNM	3.38e−237	1.29e−709	4.70e−02	2.04e−143	2.85e−428	3.10e−02
KTNM	1.86e−653	2.75e−2610	4.70e−02	3.01e−502	1.87e−2005	3.10e−02

which can be easily reduced to the following fourth-degree polynomial:

$$\psi_3(A) = A^4 - 7.79075A^3 + 14.744A^2 + 2.511A - 1.674. \tag{64}$$

Since the degree of the above polynomial is four, so, it must have exactly four roots. By definition, the fraction conversion lies in $(0, 1)$, so only one positive real root exists in this interval which is $A^* = 0.2777595428$. The other three roots have no physical meanings. The numerical results for the model (64) are shown in Table 8, wherein the optimal proposed method having fourth-order convergence, in six iterations, surpasses other methods chosen for comparison irrespective of the initial guess.

Problem 4 Planck's blackbody radiation law [22].

Plank's radiation law, also known as Planck's blackbody radiation law, describes the spectral density of electromagnetic radiation emitted by a blackbody in thermal equilibrium at a given temperature. The law states that the spectral radiance of a blackbody, or the amount of radiation emitted per unit area per unit solid angle per unit frequency, is proportional to the frequency of the radiation and the temperature of the blackbody and is given by the following equation:

$$\psi_4(w) = \exp(-w) + \frac{w}{5} - 1, \tag{65}$$

where w stands for the maximal wavelength.

Table 9 Comparison of optimal fourth-order method for Problem 4 taking $N = 6$ iterations and $TFE = 18$

Method	$\frac{\|w_n - w_{n-1}\|}{w_0 = 0.25}$	$\|\psi(w_n)\|$	Time (s)	$\frac{\|w_n - w_{n-1}\|}{w_0 = 0.45}$	$\|\psi(w_n)\|$	Time (s)
PONM	3.69e−724	5.55e−2895	1.2500e−01	4.68e−420	1.44e−1678	9.40e−02
KJNM	–	Diverge	–	2.73e−252	2.66e−1007	4.70e−02
OWNM	–	Diverge	–	–	Diverge	–
OZNM	4.78e−282	9.07e−846	7.80e−02	1.78e−283	4.73e−850	6.30e−02
KTNM	–	Diverge	–	–	Diverge	–

Table 10 Comparison of optimal fourth-order method for Problem 5 taking $N = 11$ iterations and $TFE = 22$

$[x_{1,0}, x_{2,0}]^T$	$||\mathbf{x_n} - \mathbf{x_{n-1}}||_\infty$	$[x_1, x_2]^T$	Time (s)
−0.3,−0.3	7.9406e−462	7.0058e−923, 7.0058e−923	7.6600e−01
0.2,0.2	1.5886e−673	2.8042e−1346, 2.8042e−1346	1.1560e+00
0.4,0.4	4.2299e−369	1.9880e−737, 1.9880e−737	1.1250e+00

The exact solution of (65) is 0.0. The numerical results for the model (65) are shown in Table 9, wherein the optimal proposed method having fourth-order convergence, in six iterations, surpasses other methods chosen for comparison irrespective of the initial guess.

Problem 5 The non-linear system of two equations from [1] is given as follows:

$$x_1 + \exp(x_2) - \cos(x_2) = 0,$$
$$3x_1 - x_2 - \sin(x_1) = 0. \tag{66}$$

The exact solution of the system (66) is $[0, 0]^T$.

For the computation of the error term, we use the infinity norm as $\varepsilon_n = ||\mathbf{x_n} - \mathbf{x_{n-1}}||_\infty$. The numerical simulations are shown in Table 10 for the system (66), while assuming three different guesses. It is observed that the optimal proposed method (18) gives promising results and approaches to the exact solution in eleven iterations. In other words, the approximate root at the eleventh iteration is $\approx [0, 0]^T$ for each choice of the initial guess.

8 Concluding remarks with future directions

The optimal iterative algorithm has shown improved fourth-order accuracy in both local and semilocal convergence analysis. The results of this study suggest that the optimal algorithm is efficient and accurate, and it is expected that it will continue to be developed and refined in the future. Some numerical measures including an average number of iterations, convergence area index, and generation time are taken into consideration while analyzing the performance of the proposed and other methods with polynomiographs. Overall, this work highlights the importance of developing optimal algorithms and opens up some possibilities for research in this field. Further research can be conducted to explore its potential applications in a wider range of fields and to optimize its performance even further. It is possible that this algorithm might be combined with other methods to produce a more powerful and all-encompassing approach to solving a wide range of non-linear equations.

writing—review and editing. Krzysztof Gdawiec: conceptualization, formal analysis, investigation, software, visualization, writing—original draft, writing—review and editing. Asif Ali Shaikh: writing—review and editing. Evren Hincal: writing—review and editing.

Declarations

Ethical approval Not applicable

Conflict of interest The authors declare no competing interests.

References

1. Abro, H., Shaikh, M.: A new time-efficient and convergent nonlinear solver. Appl. Math. Comput. **355**, 516–536 (2019). https://doi.org/10.1016/j.amc.2019.03.012
2. Andreev, F., Kalantari, B., Kalantari, I.: Measuring the average performance of root-finding algorithms and imaging it through polynomiography. In: Proceedings of 17th IMACS World Congress, Scientific Computation, Applied Mathematics and Simulation. Paris, France (2005)
3. Ardelean, G., Cosma, O., Balog, L.: A comparison of some fixed point iteration procedures by using the basins of attraction. Carpathian J. Math. **32**(3), 277–284 (2016)
4. Argyros, I.: Unified convergence criteria for iterative Banach space valued methods with applications. Mathematics **9**(16), 1942 (2021). https://doi.org/10.3390/math9161942
5. Argyros, I., Szidarovszky, F.: The theory and applications of iteration methods. CRC Press, Boca Raton (1993)
6. Awadalla, M., Qureshi, S., Soomro, A., Abuasbeh, K.: A novel three-step numerical solver for physical models under fractal behavior. Symmetry **15**(2), 330 (2023). https://doi.org/10.3390/sym15020330
7. Burden, R., Faires, J., Burden, A.: Numerical analysis, 10th edn. Cengage Learning Inc., Boston (2015)
8. Gdawiec, K., Kotarski, W., Lisowska, A.: On the robust Newton's method with the Mann iteration and the artistic patterns from its dynamics. Nonlinear Dynamics **104**(1), 297–331 (2021). https://doi.org/10.1007/s11071-021-06306-5
9. Jaiswal, J.: Semilocal convergence of a computationally efficient eighth-order method in Banach spaces under w-continuity condition. Iranian J. Sci. Technol. Trans. A: Sci. **42**(2), 819–826 (2018). https://doi.org/10.1007/s40995-016-0115-7
10. Jamali, K., Solangi, M., Qureshi, S.: A novel hybrid iterative method for applied mathematical models with time-efficiency. J. Appl. Math. Comput. Mech. **21**(3), 19–29 (2022). https://doi.org/10.17512/jamcm.2022.3.02
11. Jisheng, K., Yitian, L., Xiuhua, W.: A composite fourth-order iterative method for solving non-linear equations. Appl. Math. Comput. **184**(2), 471–475 (2007). https://doi.org/10.1016/j.amc.2006.05.181
12. Kalantari, B.: Polynomial root-finding and polynomiography. World Scientific, Singapore (2009). https://doi.org/10.1142/6265
13. Kantorovich, L., Akilov, G.: Functional analysis in normed spaces. Pergamon Press, Oxford (1964)
14. King, R.: A family of fourth order methods for nonlinear equations. SIAM J. Numeric. Anal. **10**(5), 876–879 (1973). https://doi.org/10.1137/0710072

15. Kung, H., Traub, J.: Optimal order of one-point and multipoint iteration. J. ACM **21**(4), 643–651 (1974). https://doi.org/10.1145/321850.321860

16. Luk, W.: Finding roots of a real polynomial simultaneously by means of Bairstow's method. BIT Numeric. Math. **36**(2), 302–308 (1996). https://doi.org/10.1007/BF01731985

17. Noor, K., Noor, M.: Predictor-corrector Halley method for nonlinear equations. Appl. Math. Comput. **188**(2), 1587–1591 (2007). https://doi.org/10.1016/j.amc.2006.11.023

18. Noor, M., Khan, W., Noor, K., Al-Said, E.: Higher-order iterative methods free from second derivative for solving nonlinear equations. Int. J. Phys. Sci. **6**(8), 1887–1893 (2011). https://doi.org/10.5897/IJPS11.425

19. Özban, A.: Some new variants of Newton's method. Appl. Math. Lett. **17**(6), 677–682 (2004). https://doi.org/10.1016/S0893-9659(04)90104-8

20. Petković, I., Rančić, L.: Computational geometry as a tool for studying root-finding methods. Filomat **33**(4), 1019–1027 (2019). https://doi.org/10.2298/FIL1904019P

21. Potra, F., Ptak, V.: Nondiscrete induction and iterative processes. Pitman Advanced Publishing Program, Boston (1984)

22. Qureshi, S., Ramos, H., Soomro, A.: A new nonlinear ninth-order root-finding method with error analysis and basins of attraction. Mathematics **9**(16), 1996 (2021). https://doi.org/10.3390/math9161996

23. Qureshi, S., Soomro, A., Shaikh, A., Hincal, E., Gokbulut, N.: A novel multistep iterative technique for models in medical sciences with complex dynamics. Comput. Math. Methods Med. **2022**, Article ID 7656451 (2022). https://doi.org/10.1155/2022/7656451

24. Rehman, M., Naseem, A., Abdeljawad, T.: Some novel sixth-order iteration schemes for computing zeros of nonlinear scalar equations and their applications in engineering. J. Function Spaces **2021**, Article ID 5566379 (2021). https://doi.org/10.1155/2021/5566379

25. Sihwail, R., Solaiman, O., Ariffin, K.: New robust hybrid Jarratt–Butterfly optimization algorithm for nonlinear models. J. King Saud University – Comput. Inf. Sci. **34**(10), 8207–8220 (2022). https://doi.org/10.1016/j.jksuci.2022.08.004

26. Sihwail, R., Solaiman, O., Omar, K., Ariffin, K., Alswaitti, M., Hashim, I.: A hybrid approach for solving systems of nonlinear equations using Harris hawks optimization and Newton's method. IEEE Access **9**, 95791–95807 (2021). https://doi.org/10.1109/ACCESS.2021.3094471

27. Solaiman, O., Hashim, I.: Optimal eighth-order solver for nonlinear equations with applications in chemical engineering. Intell. Auto. Soft Comput. **27**(2), 379–390 (2021). https://doi.org/10.32604/iasc.2021.015285

28. Solaiman, O., Sihwail, R., Shehadeh, H., Hashim, I., Alieyan, K.: Hybrid Newton-Sperm swarm optimization algorithm for nonlinear systems. Mathematics **11**(6), 1473 (2023). https://doi.org/10.3390/math11061473

29. Xiaojian, Z.: Modified Chebyshev-Halley methods free from second derivative. Appl. Math. Comput. **203**(2), 824–827 (2008). https://doi.org/10.1016/j.amc.2008.05.092

Publisher's Note Springer Nature remains neutral with regard to jurisdictional claims in published maps and institutional affiliations.

Authors and Affiliations

Sania Qureshi[1,2,3] (iD) · **Ioannis K. Argyros**[4] (iD) · **Amanullah Soomro**[1] (iD) · **Krzysztof Gdawiec**[5] (iD) · **Asif Ali Shaikh**[1,2] (iD) · **Evren Hincal**[2] (iD)

Sania Qureshi
sania.shahid@lau.edu.lb

Ioannis K. Argyros
iargyros@cameron.edu

Amanullah Soomro
amanullah.soomro@faculty.muet.edu.pk

Asif Ali Shaikh
asif.shaikh@faculty.muet.edu.pk

Evren Hincal
evren.hincal@neu.edu.tr

[1] Department of Basic Sciences and Related Studies, Mehran University of Engineering and Technology, Jamshoro 76062, Pakistan

[2] Department of Mathematics, Near East University, 99138 Mersin, Turkey

[3] Department of Computer Science and Mathematics, Lebanese American University, Beirut P.O. Box 13-5053, Beirut, Lebanon

[4] Department of Computing and Mathematics Sciences, Cameron University, Lawton, OK 73505, USA

[5] Institute of Computer Science, University of Silesia in Katowice, Bedzinska 39, 41-200 Sosnowiec, Poland